Planet. Space Sci., Vol. 30, No. 11, pp. 1083–1089, 1982
Printed in Great Britain.

0032-0633/82/111083-07$03.00/0
Pergamon Press Ltd.

THE THERMOSPHERIC HEATING EFFICIENCY UNDER ELECTRON PRECIPITATION CONDITIONS

V. SINGH and J.-C. GÉRARD
Institut d'Astrophysique, Université de Liège, 4200, Liège, Belgium

(*Received in final form* 2 *April* 1982)

Abstract—A time-dependent model calculation of the interaction between energetic electrons and the thermosphere is performed to evaluate the heating efficiency. All energy channels which contribute to the neutral heating of the atmosphere are considered in detail. Neutral chemical reactions and deactivation of metastables are found to be the major heat sources. It is shown that, below 150 km, the heating efficiency is on the order of 60% and nearly independent of altitude. At higher altitude, its value decreases in a manner depending on the atmosphere density and composition. It is concluded that, in the dayside polar cusp, particle heating may be an important source of thermospheric motion.

1. INTRODUCTION

The magnetospheric electrons precipitated in the Earth's atmosphere lose their kinetic energy by elastic and inelastic collisions with the atmospheric constituents. This energy is expended in ionization, dissociation, excitation of electronic, vibrational and rotational states, elastic collisions with ambient electrons and at sufficiently high energy, X-ray emission by bremsstrahlung. A substantial fraction of the energy deposited locally ultimately heats the neutral gas through various channels, another part escapes under the form of u.v., visible and i.r. radiation and the remaining part is stored temporarily as chemical energy released subsequently.

Another important heat source from the magnetosphere is Joule heating produced by the friction of ions and electrons accelerated under the effect of large perpendicular electric fields present at high latitudes. When integrated vertically, the two heat sources are found to be of nearly equal magnitude and strongly dependent on magnetic activity. A maximum in the general background is observed in the early afternoon and late morning regions (Banks *et al.*, 1981). Joule heating in the nightside auroral oval peaks at higher altitudes than particle heating (Banks, 1977). Therefore, the heat input/gas particle is larger by Joule than particle heating. Consequently, the vertical upwelling and subsequent large scale meridional circulation are mostly set up due to the energy released by Joule heating (Roble *et al.*, 1977; Roble *et al.*, 1981). In the dayside polar cusp, the energy of the primary electrons is usually much lower than on the nightside and the particles deposit their energy at higher altitude. Consequently, the altitude distributions of particle and Joule heating become quite similar and particle heating may become a major heat source in the dayside high latitude.

The importance of particle precipitation as a source of atmospheric heating was originally suggested by Bates (1951). In a calculation of the particle-induced composition changes, Hays *et al.* (1973) assumed that the bulk of this heating was provided by ionic recombination and used a heating efficiency of 30%. Rees (1975) discussed the energy budget of the auroral electrons and concluded that at least 60% of the electron kinetic energy heats the neutral atmosphere. However, that study was based on cross sections and rate coefficients some of which have recently undergone important revisions. Besides, the altitude distribution of the various heat sources was not examined.

In this paper, we describe the results of a study of the altitude distribution of particle heating with updated chemistry and consideration of energy fluxes typical of day- as well as night-side precipitation. This study requires the development of a time-dependent model aurora, the computation of all energy degradation processes and subsequent adding of all channels transfering kinetic energy to the neutral atmospheric constituents.

2. THE MODEL

The procedure to calculate the ionization rate and the individual ion production and dissociation rates is similar to that described by Gérard and Rusch (1979) and Rusch and Gérard (1980). In this model, we adopt quantum yields of $N(^4S)$, $N(^2D)$ and $N(^2P)$ from electron impact dissociation of 0.2,

0.7 and 0.10 respectively. This partition gives good agreement with 5200 A and 3466 A auroral observations (Rusch and Gérard, 1980; Gérard and Harang, 1980) as well as measurements of the E-region nitric oxide density (Rusch *et al.*, 1975). It is however at variance with the branching ratio of 0.45:0.35:0.20 given by Zipf *et al.* (1980) based on their laboratory studies of N_2 dissociation by electron impact. The adopted branching ratio for impact ionization of atomic oxygen is 48% $O^+(^4S)$, 32% $O^+(^2D)$ and 20% $O^+(^2P)$ (Torr and Torr, 1978). We use the neutral atmospheric composition and temperature measured in the auroral zone by Rees *et al.* (1977) by combining high altitude data from the Atmosphere Explorer C neutral mass spectrometer with observations at lower altitudes. Below 110 km, the densities are smoothly connected to the US standard Atmosphere (1977) assuming diffusive equilibrium. This atmosphere is richer in O_2 and poorer in O than the MSIS model (Hedin *et al.*, 1977) corresponding to the observed N_2 profile. This large O_2/O ratio probably indicates that the atmosphere is adjusting to auroral heating and induced vertical winds.

The system of 16 continuity equations is solved time dependently using the method described by Gérard and Barth (1977). The species considered in this computation are $O^+(^4S)$, $O^+(^2D)$, $O^+(^2P)$, O_2^+, N_2^+, N^+NO^+, electrons, $N(^4S)$, $N(^2D)$, $N(^2P)$, $O(^1D)$, $O(^1S)$ and $N_2(A^2\Sigma)$. The reactions and their rate coefficients are listed in Table 1 and are taken from the review by Torr and Torr (1978) and the study by Torr *et al.* (1980). The differential secondary electron flux is calculated at each altitude step assuming local energy loss. The energy spectrum of the ejected secondary and higher order electrons is calculated from the ionization rates using the shape factors measured by Opal *et al.* (1971). The electron-neutral loss functions and cross sections in N_2, O_2 and O are adopted from the revised values of Gattinger and Vallance-Jones (1979) and are consistent with the recent cross sections derived by Cartwright *et al.* (1977). The electron–electron loss term is described by the expression given by Swartz *et al.* (1971).

The calculated secondary electron spectrum is very similar in shape and magnitude to the results of Jones and Rees (1973) and Vallance-Jones (1975). The excitation rates of $O(^1D)$, $O(^1S)$, $N_2(A^3\Sigma)$, $N_2(B^3\pi)$ and $N_2(C^3\pi)$ by electron impact are calculated by integrating the differential electron flux on the appropriate excitation cross section. Cascading between the C, B and A states of N_2 is calculated using relevant transition probabilities and Franck–Condon factors as described by Vallance-Jones (1975). Three sources of $O(^1D)$ atoms are taken into account: excitation by electron impact on ground state atoms, dissociative recombination of O_2^+ (R11) and energy transfer between $N(^2D)$ and O_2 (R23). A branching ratio of 1.3, consistent with the airglow measurements of Hays *et al.* (1978), is used for the production of $O(^1D)$ by reaction 11. Reaction 23 is assumed to produce only $O(^1D)$ atoms, in agreement with the conclusion by Rusch *et al.* (1978). The role of this reaction as a source of $O(^1D)$ atoms is not firmly established and its efficiency is currently under debate (Link *et al.*, 1981; Torr *et al.*, 1981). The importance of the yield of $O(^1D)$ by R23 will be discussed below.

The electron temperature profile is calculated by solving numerically the heat equation of the electrons. The heat source is the collisions between superthermal and thermal electrons and is given by the expression:

$$Q_e(z) = \int_0^\infty \left(\frac{dE_s}{dx}\right)_{e-e} \Phi(E_s, z)\, dE_s,$$

where $(dE_s/dx)_{e-e}$ is the stopping power of electrons by secondary electrons at altitude z and $\Phi(E_s, z)$ the secondary electron flux. The electron cooling terms are shown in Fig. 1 for the case of a 10 erg cm^{-2} s^{-1} precipitation with $\alpha = 2$ keV, where α is the characteristic energy of primary electrons in a Maxwellian distribution. The expressions are taken from Banks and Kockarts (1973) with the exception of the N_2 vibrational term which is from

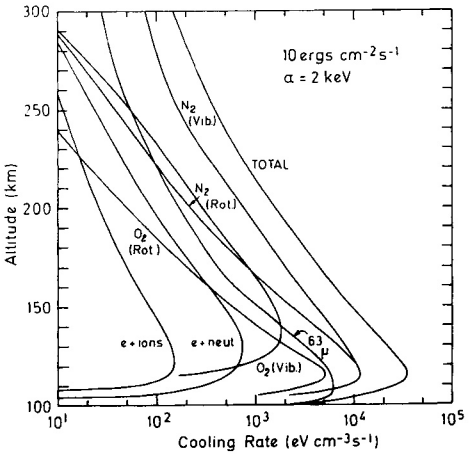

FIG. 1. COOLING RATES OF THERMAL ELECTRONS FOR A MODEL AURORA CHARACTERIZED BY A MAXWELLIAN DISTRIBUTION WITH $\alpha = 2$ keV AND 10 erg cm^{-2} s^{-1} ENERGY INPUT.

TABLE 1. CHEMICAL REACTIONS

Reaction number	Reactions	Rate coefficient ($cm^3 s^{-1}$)	Exothermicity (eV)
R1	$O^+(^2D) + N_2 \rightarrow N_2^+ + 0$	7.0×10^{-11}	1.33
R2	$O^+(^2D) + N_2 \rightarrow O^+ + N_2$	3.0×10^{-11}	3.31
R3	$O^+(^2D) + e \rightarrow O^+ + e$	$7.8 \times 10^{-8}(Te/300)^{0.5}$	3.31
R4	$O^+(^2P) + e \rightarrow O^+(^2D) + e$	$1.5 \times 10^{-7}(Te/300)^{0.5}$	1.69
R5	$O^+(^2P) + O \rightarrow O^+ + O$	5.2×10^{-10}	5.00
R6	$O^+(^2P) + N_2 \rightarrow N_2^+ + O$	4.8×10^{-10}	3.02
R7	$O^+ + O_2 \rightarrow O_2^+ + O$	$2.0 \times 10^{-11}(Te/300)^{-0.4}$	1.55
R8	$O^+ + N_2 \rightarrow NO^+ + N$	$1.2 \times 10^{-12}(Ti/300)^{-1.0}$	1.10
R9	$O_2^+ + NO \rightarrow NO^+ + O_2$	4.4×10^{-10}	2.81
R10	$O_2^+ + e \rightarrow O + O$	$6.8 \times 10^{-8}(Te/300)^{-1.0}$	6.97
R11	$O_2^+ + e \rightarrow O(^1D) + O(^1D)$	$1.3 \times 10^{-7}(Te/300)^{-1.0}$	3.05
R12	$O_2^+ + N \rightarrow NO^+ + O$	1.8×10^{-10}	4.19
R13	$N_2^+ + e \rightarrow N(^2D) + N(^4S)$	3.0×10^{-7}	3.44
R14	$N_2^+ + O \rightarrow NO^+ + N(^2D)$	$1.4 \times 10^{-10}(Ti/300)^{-0.44}$	0.70
R15	$N_2^+ + O_2 \rightarrow N_2 + O_2^+$	6.0×10^{-11}	3.53
R16	$N^+ + O \rightarrow N + O^+$	8.0×10^{-10}	0.93
R17	$N^+ + O_2 \rightarrow O_2^+ + N(^2D)$	2.75×10^{-10}	0.11
R18	$N^+ + O_2 \rightarrow NO^+ + O$	2.8×10^{-10}	6.67
R19	$NO^+ + e \rightarrow N(^2D) + O$	$3.2 \times 10^{-7}(Te/300)^{-1.0}$	0.38
R20	$NO^+ + e \rightarrow N(^4S) + O$	$8.0 \times 10^{-8}(Te/300)^{-1.0}$	2.75
R21	$O(^1D) + N_2 \rightarrow O + N_2$	3.0×10^{-11}	1.96
R22	$N_2(A^3\Sigma) + O \rightarrow N_2 + O$	1.2×10^{-10}	6.14
R23	$N(^2D) + O_2 \rightarrow NO + O(^1D)$	5.0×10^{-12}	1.84
R24	$N(^2D) + O \rightarrow N + O$	4.0×10^{-13}	2.38
R25	$N(^2D) + e \rightarrow N + e$	$5.0 \times 10^{-10}(Te/300)^{0.5}$	2.38
R26	$N(^2D) + NO \rightarrow N_2 + O$	7.0×10^{-11}	5.66
R27	$N(^2P) + O, \rightarrow NO + O$	2.8×10^{-12}	4.96
R28	$N(^2P) + O \rightarrow N(^2D) + O$	1.0×10^{-10}	1.18
R29	$N(^2P) + e \rightarrow N + e$	$5.0 \times 10^{-10}(Te/300)^{0.5}$	3.56
R30	$N(^2P) + NO \rightarrow N_2 + O$	3.2×10^{-11}	6.84
R31	$N + NO \rightarrow N_2 (v = 5) + O$	$2.6 \times 10^{-11}(Ti/300)^{0.5}$	1.85
R32	$N + O_2 \rightarrow NO + O$	$2.4 \times 10^{-11} e^{-3975/Ti}$	1.42

Rees and Roble (1975) and the 63μ oxygen excitation given by Hoegy (1976). At high altitudes, the N_2 vibrational excitation and 63μ terms dominate but in the region of maximum deposition, the contributions of the O_2 and N_2 rotational terms are also significant. At the altitudes considered in this study, we assume $T_i = T_n$.

3. HEATING EFFICIENCY

As the primary electrons penetrate into the thermosphere, they loose kinetic energy and create secondary electrons which subsequently thermalize by collisions with ambient neutrals and electrons. Heating of the neutral atmosphere is made via three different channels: (a) direct dissociation of atmospheric molecules whose fragments carry excess kinetic energy, (b) exothermic chemical reactions involving ions, ground state and metastable neutral species, (c) cooling of thermal electrons.

In the process of dissociation of N_2 by energetic electrons, the kinetic energy lost by each primary electron is shared between the dissociation energy of the molecule, the electronic excitation of the atoms and the kinetic energy of the fragments. No laboratory measurement is available of the energy spectrum of the atoms following dissociation by electron impact. To estimate crudely this contribution, it is assumed that the nitrogen atoms carry an average kinetic energy of 0.3 eV.

Exothermic chemical reactions are of two categories. The first one is between neutral species and the other one between ions and neutrals or ions and electrons. These reactions are listed in Table 1 along with their exothermicity. The kinetic heating rate for each reaction is obtained by multiplying the reaction rate by the exothermicity. Some of these reactions involve metastable atoms or molecules which can only radiate through forbidden electronic transitions. If the metastable state is deactivated by a collision before it can radiate, the excitation energy is transfered to the neutral gas

and heats the thermosphere. Thermal electrons cool by elastic and inelastic collisions with ambient neutrals and ions. The ion gas, in turn, cools only by collisions with the neutral atmosphere and provides another source of neutral heating.

Figure 2 gives the heating rate due to neutral reactions and quenching. We have only shown processes which contribute at least 5% to the total heating rate. The altitude dependence of the major sources are illustrated at steady state for a 10 ergs cm^{-2} s^{-1} electron precipitation with a primary Maxwellian energy spectrum characterized by $\alpha = 2$ keV. The deactivation of metastable $O(^1D)$ atoms by N_2 is the major heat source, followed by the quenching of $N(^2D)$ by molecular oxygen. In the region of maximum energy deposition, quenching of $N_2(A^3\Sigma)$ also contributes a significant amount to kinetic heating. Figure 3 illustrates the heating rate due to ion-neutral reactions. At high altitude, dissociative recombination of O_2^+ and NO^+ make the major contributions but at lower altitude, $N_2^+ + O_2$ and $O_2^+ + NO$ are dominant. Comparison between Figs. 2 and 3 show that the ionic reactions contribute less than 20% to the total heating rate. Direct dissociation by electron impact contributes about 2% and electron cooling less than 1%.

The heating efficiency is obtained by dividing the total heat production rate by the rate of energy deposition at each altitude. The local electron energy loss is obtained by multiplying the total ionization rate by the average energy necessary to create an ion pair. The adopted values are 36 eV for N_2, 32 eV for O_2 and 27 eV for O, in agreement

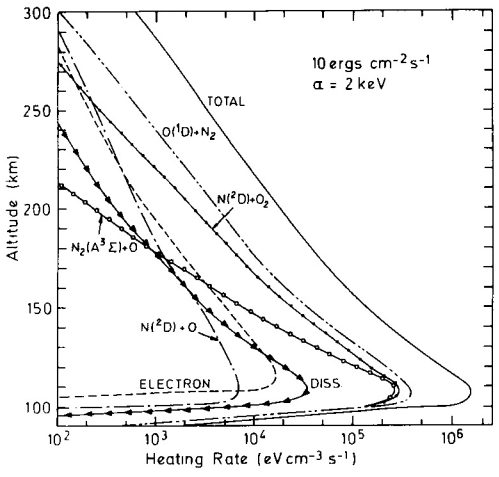

FIG. 2. KINETIC HEATING RATE DUE TO NEUTRAL CHEMICAL REACTIONS AND QUENCHING FOR THE SAME CASE AS IN FIG. 1.

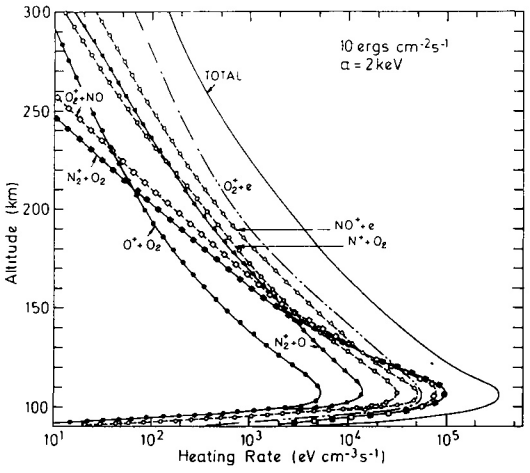

FIG. 3. KINETIC HEATING RATE DUE TO IONIC CHEMICAL REACTIONS FOR THE SAME CASE AS IN FIG. 1.

with laboratory measurements (Valentine and Curran, 1958) and theoretical calculation (Green *et al.*, 1977).

We adopted Maxwellian energy distributions with $\alpha = 2$ keV, a value typical of energies measured in the nightside auroral precipitation. The curve in Fig. 4 illustrates the results obtained from the model aurora described previously run to a steady state. The results show that the heating efficiency

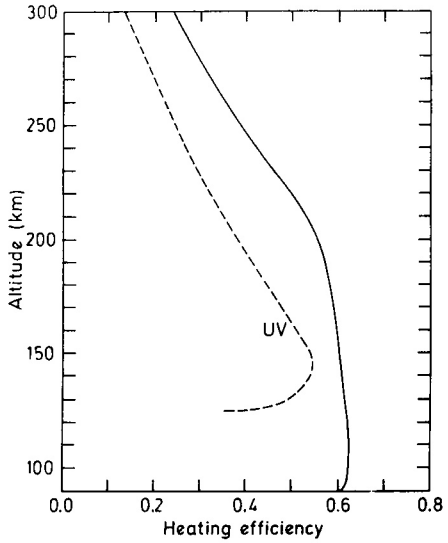

FIG. 4. ALTITUDE DISTRIBUTION OF THE HEATING EFFICIENCY FOR A MODEL AURORA (SOLID LINE). The solar u.v. heating efficiency calculated by Torr *et al.* (1980) for July 1, 1974 is also shown for comparison (dotted line).

remains nearly constant between 0.55 and 0.62 below about 200 km and independent of the energy input. At higher altitude, the efficiency curve shows a monotonic decrease. The shape of the curve is explained by the fact that the dominant heat sources are quenching reactions of metastable states. As altitude increases, the fraction of collisional radiationless transitions decreases, causing the drop in the heating efficiency. At low altitude, radiation from these metastables becomes negligible and the heating efficiency is independent of altitude. A steady state is reached within seconds or minutes for most chemical and quenching processes. However, the density of nitric oxide builds up due to the particle-induced ionization and N_2 dissociation until saturation is eventually reached.

The $N(^4S) + NO$ and $N(^2D) + NO$ recombinations (R26 and R31) involve long-lived species whose densities do not respond rapidly to the energy input and are submitted to transport. Consequently, their contribution to kinetic heating cannot be directly included in the heating efficiency calculations. Instead, they must be considered as separate terms when solving the thermodynamic energy equation.

As illustrated by Gérard and Barth (1977), when the precipitation stops or decreases, the NO recombination proceeds until $N(^4S)$ is totally depleted. The remaining nitric oxide is dissociated by u.v. solar radiation and transported downward and horizontally (Roble and Gary, 1979; Gérard and Roble, 1982). The latter process is the only loss mechanism in the case of precipitation in the polar night. Neglecting transport, we estimate from the results of our model calculation for 10 ergs cm^{-2} s^{-1} that an excess column density of 9×10^{14} NO molecules cm^{-2} is left after 1 h of precipitation, corresponding to a chemical energy storage of 2.7×10^3 ergs cm^{-2}. Comparing this figure to a time-integrated input of 3.6×10^4 ergs cm^{-2}, we deduce that in this case, about 7% of the total precipitated energy is stored under the form of odd nitrogen. This fraction may be compared with the 3% instantaneous contribution provided by the N + NO recombination. As mentioned before, the yield of $N(^2D)$ atoms by reaction 23 has not been determined experimentally but a high efficiency was assumed by Rusch *et al.* (1978). The present calculations assumed a 100% branching ratio. If, instead, only $O(^3P)$ atoms are produced, the energy released is 3.80 eV instead of 1.84 eV. Consequently, the effect of this branching ratio may be calculated by comparing the heat produced by the chain of reactions:

$$N(^2D) + O_2 \rightarrow NO + O(^1D) + 1.84\ \text{eV}$$

$$O(^1D) + N_2 \rightarrow O(^3P) + N_2 + 1.96\ \text{eV}$$

$$O(^1D) \rightarrow O(^3P) + \lambda 6300\text{A}$$

to:

$$N(^2D) + O_2 \rightarrow NO + O(^3P) + 3.80\ \text{eV}.$$

The ratio of heat production of the two paths is given by:

$$R = 0.48 + 0.52 \frac{k_{21}[N_2]}{A_{6300} + k_{21}[N_2]},$$

where A_{6300} is the $[OI]^3P$–^1D transition probability and k_{21} the quenching coefficient of $O(^1D)$ by N_2. The ratio R varies from 0.48 for negligible quenching to 1 when quenching dominates over radiation. With the model atmosphere used in this study, R is about 0.7 at 300 km and the corresponding change in total heating rate is about 1%. Consequently, the choice of the branching ratio for reaction R21 is of little effect on the calculated heating efficiency for the range of altitudes considered here.

The choice of the branching ratio for the production of $N(^2D)$ atoms by electron impact dissociation of N_2 has some influence on the calculated heating efficiency since the metastable atoms carry some 2.96 eV excitation energy. At altitudes where quenching completely dominates, the supplement energy carried by the $N(^2D)$ atoms produced by electron impact on N_2 is $2.96\ 2f\ D(N_2)$, where f is the effective fraction of $N(^2D)$ and $D(N_2)$ the dissociation rate of N_2. Consequently, the difference in heating efficiency is $2.96\ 2f\ 0.6/35 = 0.1f$, since the dissociation rate is about 0.6 times the ionization rate and 35 eV are expended to create an ion pair. Thus, for example, varying f from 80% (this model) to 50% would decrease the heating efficiency by about 3% at low altitudes. Actually, the situation is more complex since a large fraction of $N(^2D)$ atoms react with O_2 to form NO molecules which may be transported by diffusion and winds. The heating of the atmosphere by solar u.v. radiation has been studied by Stolarski *et al.* (1975) and Torr *et al.* (1980). The latter found that, out of the incident energy input of 1.47 ergs cm^{-2} s^{-1}, 50–55% is channelled into neutral heating. For comparison, their heating efficiency curve for July 1, 1974 is plotted in Fig. 4. The absolute value of the heating efficiency and its altitude distribution vary significantly with the solar cycle and to a minor extent, with the season.

Above 200 km, the u.v. and the particle curves are nearly parallel. The u.v. efficiency peaks near 150 km and drops below this altitude. The relative importance of the heat sources plotted in Figs. 2 and 3 is very similar to the solar heating case. However two major factors explain the differences between the two cases:

(i) the O_2 dissociation in the Schumann–Runge continuum which represents 33% of the solar energy input, makes no contribution in the particle precipitation case and

(ii) the partition of energy between the various channels is different in the case of u.v. photons and energetic electrons.

4. CONCLUSIONS

The auroral model described above has been used to study the heating efficiency of the neutral atmosphere submitted to energetic electron precipitation. The calculations indicate that more than 60% of the energy input produces heating of the neutral gas in the case of electrons depositing most of their energy in the lower thermosphere. For a softer precipitation such as observed in the dayside cusp, the heating efficiency is lower and depends on the energy of the precipitation. Satellite and rocket measurements made through the cusp have indicated that the particle energy flux varies between a fraction to a few ergs $cm^{-2} s^{-1}$ (Potemra *et al.*, 1977 and references therein). Combining these values with our results, we conclude that the corresponding particle heating may exceed 1 erg $cm^{-2} s^{-1}$ and becomes comparable to the rate of Joule heating observed in the dayside cusp. Since the altitude distribution of both heat sources is also similar for soft precipitation, the effect of particle heating may become significant as a driver of vertical and meridional circulation.

Note added in proof

After completion of the manuscript, measurements of the kinetic energy of the fragments of the N_2 dissociation by electron impact were reported by Prokop and Zipf (1982) (*EOS Trans. AGU* **18**, 393). They found that the mean energy of the N atoms is 0.45 eV for dissociation and 3 eV for dissociative ionization. Considering the relative importance of the two processes, an average energy of about 1 eV is carried as kinetic energy of the nitrogen atoms. If this value is used instead of the arbitrary value quoted in the text, the curve labelled "dissociation" in Fig. 2 should be increased by a factor of 3, thus making the contribution of N_2 dissociation 6% of the total heating rate.

Acknowledgements—One of the authors (JCG) is supported by the Belgian National Foundation for Scientific Research (FNRS). V. Singh is grateful to the University of Liège for a research followship. This research was supported by FRFC grant Nr. 2.4507.82.

REFERENCES

Bates, D. R. (1951). *Proc. Phys. Soc.* **B64**, 805.
Banks, P. M. (1977). *J. atmos. terr. Phys.* **39**, 179.
Banks, P. M., Foster, J. C. and Doupnik, J. R. (1981). *J. geophys. Res.* **86**, 6869.
Banks, P. M. and Kockarts, G. (1973). *Aeronomy*, part B. Academic Press, New York.
Cartwright, D. C., Trajmar, S., Chutjan, A. and Williams, W. (1977). *Phys. Rev.* **A16**, 1041.
Gattinger, R. L. and Jones, A. V. (1979). *Planet. Spac Sci.* **27**, 169.
Gérard, J. C. and Barth, C. A. (1977). *J. geophys. Res.* **82**, 674.
Gérard, J. C. and Harang, O. E. (1980). *J. geophys. Res.* **85**, 1757.
Gérard, J. C. and Rusch, D. W. (1979). *J. geophys. Res.* **84**, 4335.
Gérard, J. C. and Roble, R. G. (1982). *Planet. Space Sci.* **30**, 1091.
Green, A. E. S., Jackman, C. H. and Garvey, R. H. (1977). *J. geophys. Res.* **82**, 5104.
Hays, P. B., Jones, R. A. and Rees, M. H. (1973). *Planet. Space Sci.* **21**, 559.
Hays, P. B., Rusch, D. W., Roble, R. G. and Walker, J. C. G. (1978). *Rev. Geophys. Space Phys.* **16**, 225.
Hedin, A. E., Reber, C. A., Newton, G. P., Spencer, N. W., Brinton, H. C., Mayer, H. G. and Potter, W. E. (1977). *J. geophys. Res.* **82**, 2148.
Hoegy, W. R. (1976). *Geophys. Res. Lett.* **3**, 541.
Jones, R. A. and Rees, M. H. (1973). *Planet. Space Sci.* **21**, 537.
Link, R., McConnell, J. C. and Shepherd, G. G. (1981). *Planet. Space Sci.* **29**, 589.
Opal, C. B., Peterson, W. K. and Beaty, E. C. (1971). *J. Chem. Phys.* **65**, 154.
Potemra, T. A., Peterson, W. K., Doering, J. P., Bostrom, C. O., McEntre, R. W. and Hoffman, R. A. (1977). *J. geophys. Res.* **82**, 4765.
Rees, M. H., Stewart, A. I., Sharp, W. E., Hays, P. B., Hoffman, R. A., Brace, M. H., Doering, J. P. and Peterson, W. K. (1977). *J. geophys. Res.* **82**, 2250.
Rees, M. H. and Roble, R. G. (1975). *Rev. Geophys. Space Phys.* **13**, 201.
Rees, M. H. (1975). *Planet. Space Sci.* **23**, 1589.
Roble, R. G. and Gary J. M. (1979). *Geophys. Res. Lett.* **6**, 703.
Roble, R. G., Dickinson, R. E. and Ridley, E. C. (1977). *J. geophys. Res.* **82**, 5493.
Roble, R. G., Dickinson, R. E. and Ridley, E. C. (1981). *J. geophys. Res.* **87**, 1599.
Rusch, D. W., Stewart, A. I., Hays, P. B. and Hoffman, J. H. (1975). *J. geophys. Res.* **80**, 2300.
Rusch, D. W. and Gérard J. C. (1980). *J. geophys. Res.* **85**, 1285.
Rusch, D. W., Gérard, J. C. and Sharp, W. E. (1978). *Geophys. Res. Lett.* **5**, 1043.

Stolarski, R. S., Hays, P. B. and Roble, R. G. (1975). *J. geophys. Res.* **80**, 2266.
Swartz, W. E., Nisbet, J. S. and Green, A. E. S. (1971). *J. geophys. Res.* **76**, 8425.
Torr, D. G. and Torr, M. R. (1978). *Rev. Geophys. Space Phys.* **16**, 327.
Torr, M. R., Richards, P. G. and Torr, D. G. (1980). *J. geophys. Res.* **85**, 6819.
Torr, D. G., Richards, P. G., Torr, M. R. and Abreu, V. J. (1981). *Planet. Space Sci.* **29**, 595.
U.S. Standard Atmosphere (1976). NOAA, NASA & USAF, NOAA-S/T 86, 1562.
Valentine, J. M. and Curran, S. C. (1958). *Rep. Prog. Phys.* **21**, 1.
Vallance-Jones, A. (1974). *Aurora.* D. Reidel, Dordrecht, Holland.
Zipf, E. C., Espy, P. J. and Boyle, C. F. (1980). *J. geophys. Res.* **85**, 687.